International Research Journal of Innovations in Engineering and Technology (IRJIET)

ISSN (online): 2581-3048
Volume 9, Issue 8, pp 75-80, August-2025
https://doi.org/10.47001/IRJIET/2025.908010

To Understand the Capabilities of Doppler Radar

[1]Sadhan Biswas, [2]Dr. Devendra Pradhan

[1]Ph.D Scholar, Department of Physics, Mansarovar Global University, Sehore - 466111, Madhya Pradesh, India
[2]Professor, Department of Physics, Mansarovar Global University, Sehore - 466111, Madhya Pradesh, India
Authors E-mail: [1]sadhanphy@gmail.com, [2]pradhandev1960@gmail.com

***Abstract* - Heavy rainfall, lightning, strong thunderstorms, and hailstorms are common in the Gangetic West Bengal region, making it an ideal location to research these phenomena before the monsoon season. Tropical cyclones and other bigger systems also make landfall in this region before and after the monsoons, wreaking havoc along the Bay of Bengal coasts of Bangladesh, Orissa, and West Bengal. The study of these weather phenomena has made substantial use of satellite and analog weather radars during the past few decades, among other observational techniques. But with the advent of Doppler Weather Radar (DWR), precision and quantitative in observations were both enhanced. Doppler weather radar applications from Kolkata, India, encompassing an area 400 km in diameter and including the whole Gangetic West Bengal region, formed the backbone of the author's work. Tropical cyclones and thunderstorms that formed in the Gangetic, West Bengal area have been the primary focus of structural investigation. Doppler radar products may be done rather accurately at least 2-3 hours in advance. While DWR data is useful, analyzing and using the convective indices may further enhance the lead time of now casting.**

Keywords: Environmental, Atmospheric, Doppler, Radar and Meteorological.

I. INTRODUCTION

Radar systems have been more important in military, meteorological, and navigational uses for quite some time. Collision avoidance, bearing and speed computations, range, aerial interception, and many other uses have made radar systems ubiquitous in maritime and aviation navigation equipment, whether utilised by the military or civilians. Weather conditions including rain, snow, and storms may be predicted with the use of specialized Doppler radar equipment in meteorology. Surveillance, target recognition, and tracking are just a few of the defense applications that have recently garnered the greatest attention for radar systems. Surveillance and perimeter defense are two areas that have recently shown interest in the challenge of target detection utilizing radar devices. The objective of these kinds of issues is to identify and differentiate various targets by analyzing the radar system's reception of the echo signals that these objects bounce back to it. Any moving item inside the radar's detection range is considered a target in this context.

The main thing that goes into a watershed system is precipitation. Accurate geographical and temporal measurements of the precipitation input are prerequisites for conducting hydrologic analyses with certainty. Presently, rainfall is being measured at discrete points in the field using rain gauges. However, when these point values are extrapolated to provide distributions for the skies, spatial variation is missing. Because of the large spatial and temporal variability in precipitation, the reliability of runoff and flood predictions would suffer if the watershed had just a small number of rain gauge stations.

Several hydrological models were created in the past with the assumption that rainfall is uniform over a region; nevertheless, the outcomes of these models often contradicted the data that was actually observed. A dense rain gauge network is ideal for accurately estimating a watershed's rainfall and runoff, but it's expensive to set up and keep running (Mapiam et al., 2009). According to Suresh (2010), a dense network of 2 km x 2 km might be necessary for planning in India. Nevertheless, a feasible network of rain gauges measuring 4 km x 4 km has been suggested, due to the practical challenges. However, because to geographical and topographical limitations, financial limits, and maintenance-related issues, this network density is also practically impossible. According to Guhathakurta and Rajeevan (2008), there is now one rain gauge station for every 3402 sq. km area in India.

Observing rainfall occurrences over a vast region may be greatly assisted by meteorological long-range radars. Compared to rain gauges, radar provides superior spatial and temporal resolution when it comes to analysing precipitation patterns. According to several studies, meteorological radars provide numerous benefits over traditional rain gauges. For example, according to Wyss et al. (1990), Borga (2002), Meischner (2004), Mikayla and Paul (2005), and Eloise and Peter (2010), a single station may get coverage over a large region with excellent spatial and temporal resolution.

International Research Journal of Innovations in Engineering and Technology (IRJIET)

ISSN (online): 2581-3048

Volume 9, Issue 8, pp 75-80, August-2025

https://doi.org/10.47001/IRJIET/2025.908010

II. LITERATURE REVIEW

Ezio (2021) collected data from a station with one C-band Doppler meteorological radar and many rain gauges along the upper Reno River at Casalecchio, close to Bologna, Italy. The research only used 26 of the many available recorded rain gauges in the upper Reno River watershed. We used the Bayesian correction approach to adjust the radar and rain gauge readings. We compared the discharges recorded at Casalecchio with those predicted by a rainfall-runoff model that used rainfall data from rain gauges and radar readings. He came to the conclusion that there is a vast array of potential uses for the Bayesian approach that combines rainfall predictions from weather radar with data from rain gauges, and that the methodology that was suggested lends more credence to the radar-based rainfall estimations.

Bhatnagar et al. (2023), the basics of radar, digital signal processors, the Doppler principle, and the unique characteristics and products offered by the DWR in Chennai were summarised by. As a result of technical progress, Doppler radar became the primary information source for the general public. If a traditional rain gauge network isn't available, radar precipitation estimates may help with water inflow calculations in catchments and near-real-time flash flood predictions. To add to that, evaluating the hydrological cycle—which has major effects on temperature and climate change—can be greatly aided by radar estimate across the enormous marine region. In order to get an accurate radar precipitation, estimate, they also stressed the necessity of doing more study to determine the values of 'a' and 'b' in the Z-R relationship of DWR, Chennai for various seasons.

Using high-resolution, real-time Doppler weather radar data, Carl et al. (2020) created a system called KINEROS2 to predict flash floods in smaller basins in Southern Arizona and Central New York State. For basins with mostly overland flow, the KINEROS2 model was created to simulate the rainfall-runoff response. It is an event-oriented, distributed, physically-based model. They used data with a spatial resolution of 1 degree by 1 kilometre derived from the National Weather Service Weather Surveillance Radar 88 Doppler (NWS WSR-88D), specifically the Digital Hybrid Reflectivity (DHR) radar product, which was acquired at 4-minute intervals. The forecaster is notified by the established model if the highest forecasted stage level surpasses the crucial stage or stages that they have chosen.

Ruiz-Villanueva et al. (2022) used two German meteorological service-operated C-band Doppler radars to study the flash flood maxima in the Starzel River basin in southwestern Germany. To ensure the accuracy of the radar-based predictions, four hourly rain gauges were used. After comparing the modified radar estimations with the rain gauge data, a spatially uniform bias factor was used to scale the final rainfall accumulations. A distributed hydrological model was fed with the radar rainfall estimates in order to simulate floods and to characterize the structure and dynamics of the storm that produced the flash floods. Researchers were able to analyse the hydrometeorological and hydrological processes linked to the severe storm and subsequent flood in depth because to the availability of high-resolution radar rainfall in conjunction with a rain gauge network.

Marco et al. (2022) Research on the feasibility of using tiny, inexpensive X-band radars to track and record rainfall occurrences in an Italian hilly area with relatively narrow valleys was detailed in a recent presentation. Marco shown that inexpensive, short-wavelength radars can monitor and observe rainfall episodes independently, and they have great spatial and temporal resolution. In mountainous areas and complicated orographic terrain, X-band radars may enhance the current rain gauge networks and the widely utilised C-band and S-band long range high-power radar networks, they found, and cover a notable gap in observational meteorology.

III. VOLUME SCAN STRATEGY

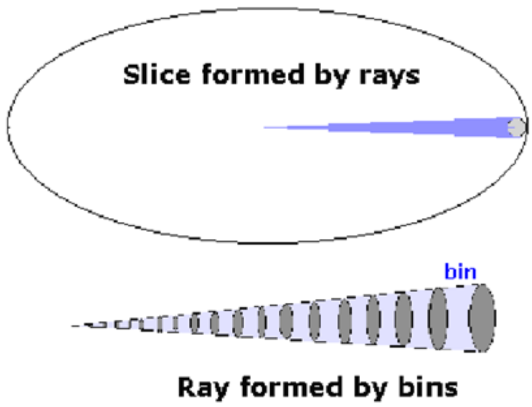

Figure 1(a)

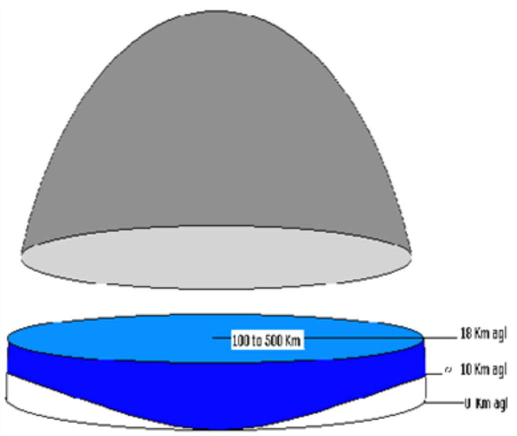

Figure 1(b)

International Research Journal of Innovations in Engineering and Technology (IRJIET)

ISSN (online): 2581-3048

Volume 9, Issue 8, pp 75-80, August-2025

https://doi.org/10.47001/IRJIET/2025.908010

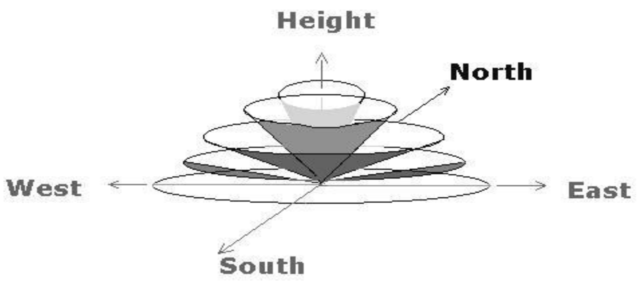

Figure 1(c)

Doppler weather radar uses an azimuth scan at varying elevation angles to gather volume data within a user-defined region. The overall plan is shown in Figure 1.

a) **Bin** - "Bin" is the name given to the smallest component of the ray that contains meteorological data. Figure 1(a) shows that the user determines the total number of bins, and the size of each bin is determined by dividing the entire range of observations by the number of bins.
b) **Ray** - The bins in figure 1(a) create a ray.
c) **Slice** - An azimuth rotational scan (3600) on a ray is used to produce the slice {fig. 1(a)}.
d) **Volume** - Volume is determined by slices taken at different elevation angles {fig. 1(b) & 1(c)}.

Each volume scan produces three data files: one for the reflectivity, one for the radial velocity, and one for the spectrum width, which are all base products. M/S Emotronic of Germany, who makes the radar, created the application program "Rainbow 3.4" to extract different products from the large raw data sets. Following is a discussion of these foundational items: - A

IV. RADAR REFLECTIVITY FACTOR (Z)

One way to quantify the amount of precipitation in a cloud system's sample volume is using this product. This product may help you understand the system's characteristics, including the quantitative estimation of the precipitation contents and rate. The Radar Reflectivity factor (Z), measured in mm6 / m3, indicates the intensity of the backscattered signal and is dependent on the amount of precipitation in the cloud. Because reflectivity factors often vary from very tiny (on the order of 10-2) to extremely high (on the order of 10^8), it is practical to represent Z on the logarithmic scale, written as dBZ, as

$$dBZ = 10 \log_{10} \{Z / (mm^6/m^3)\} \qquad (3.1)$$

$$Z = \sum D^6 \text{ per unit volume}$$

Where "D" stands for the raindrops' diameter. The program creates pseudo colors to show the reflectivity in dBZ.

V. MEAN RADIAL VELOCITY (V)

This output is an approximation of the system's mean wind speed in the direction of or away from the radar, calculated by using the Doppler Principle, which was covered in Chapter 2. Because radar can only detect wind speeds along the radar beam, which are tangential to the ground, this kind of velocity is called radial velocity.

If the system is approaching the radar along the radar beam the radial velocity towards the radar will be considered as negative and will represent the real wind velocity. However, when measured in an outward direction from the radar, the radial velocity is considered positive. If the wind is perpendicular to the radar beam, then the radial velocity will be 0.

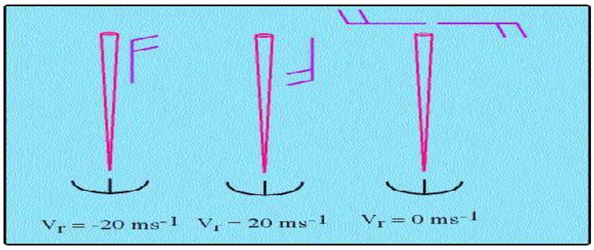

Figure 2: Radial Velocity Products

VI. STANDARD VELOCITY PRODUCTS

a) PPI_V (Plan position Indicator Velocity)

Obtaining data on radial velocities is as easy as doing an azimuth scan at a constant height using this product. Both positive and negative velocities are represented on the velocity scale. Clouds are also moving in the direction of the radar when the radial component of the wind direction is negative, which is indicated by a negative velocity. In a similar vein, positive velocities are derived from the observation that clouds are moving away from radar when the radial component of wind speed is away from the radar.

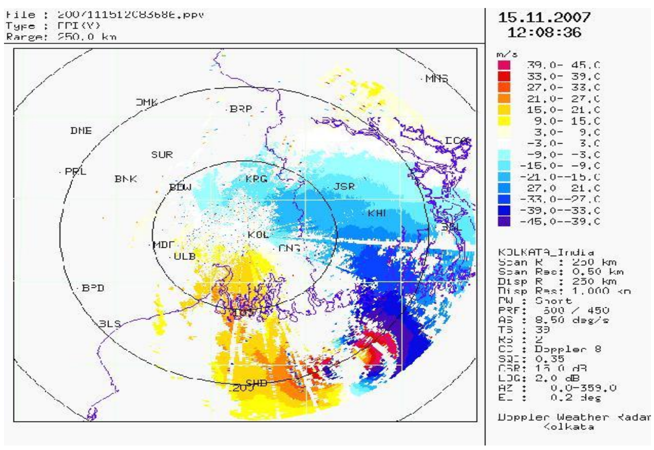

Figure 3: (15.11.2007 / 1208 UTC)

International Research Journal of Innovations in Engineering and Technology (IRJIET)

ISSN (online): 2581-3048

Volume 9, Issue 8, pp 75-80, August-2025

https://doi.org/10.47001/IRJIET/2025.908010

Figure 3 shows the PPI picture of cyclone SIDR on November 15, 2007, which shows a well-defined circular eye located around 200 km southeast of DWR in the storm's eye. Based on the high winds in the wall cloud region and the smaller wind-free area in the center, we may estimate the eye diameter and cyclone strength. You can see two sections of wall clouds in the figure. One of them has a velocity of around 51 m/s, which is calculated using the velocity unfolding concept, which is covered in Chapter 6 under cyclones. The other zone of wall clouds has a velocity of about 45 m/s. In this case, the velocity pattern depicts the cyclonic circulation around the cyclone's eye.

Description of the legends used in PPI_V

The legends provided on the right side of the image are discussed below:

a) Scan R: The range of scanning by the radar (250 km)
b) Scan Res: The resolution during scanning (0.50 km)
c) Disp R: Displayed range of the image (250 km)
d) Disp Res: Resolution of the displayed image (1 km)
e) PW short: Short pulse width of duration 1 micro second (used for radial velocity measurements)
f) PRF: Pulse Recurrence Frequency (Dual PRF technique 600:450 HZ)
g) AS: Antenna Scanning rotation rate (8.5 deg/sec)
h) TS: Time Sampling (no of samples per second collected during scanning)
i) RS: Range Sampling (no of samples considered for display of the image)
j) CC: Clutter Correction (Doppler filters to suppress the clutters)
k) SQI: Signal Quality Index (A parameter for the signal processor to control the noise and to maintain the desired level of signal, 0.35)
l) CSR: Clutter to Signal Ratio (15 dB)
m) Log: Log threshold for the desired signal above noise (2 dB)
n) Az: Azimuth movement for scanning (0.0- 359.0 deg)
o) El: Angle of elevation for observation (0.2 deg)

b) CAPPI_V (Constant Altitude PPI Velocity)

This product's methodology is almost identical to CAPPI reflectivity; the only real difference is how the data is presented. The color table illustrates the idea of velocity for this picture, which is the radial velocity, as seen in the image.

Tropical cyclone SIDR's radial velocity at 2 km altitude The data collecting range is limited to 150 kilometers at this height, for the same reason as CAPPI reflectivity. The wind is blowing anticlockwise at a magnitude of about 15 m/s, with the picture revealing that it is approaching the station from the northeast and heading southeast. The CAPPI's 2 km range is only 150 km, thus the eye and wall cloud couldn't be seen in this picture.

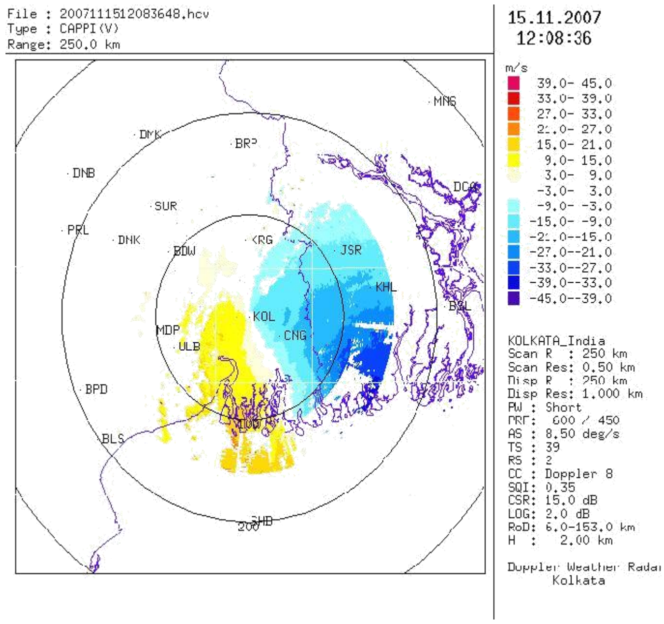

Figure 4: (15.11.2007 / 1208 UTC)

c) PCAPPI_V (Pseudo CAPPI Velocity)

The only difference between this product and the PCAPPI reflectivity test is how the radial velocity is shown on the color scale.

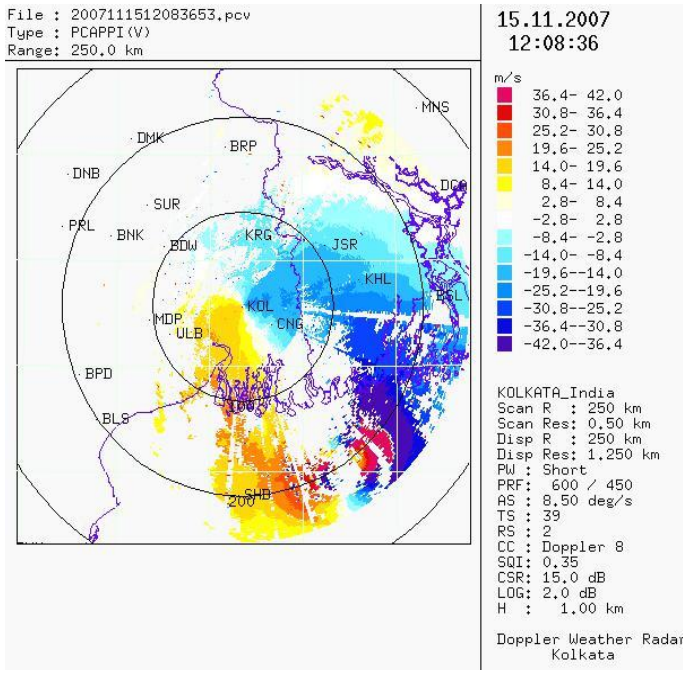

Figure 5: (15.11.2007 / 1208 UTC)

International Research Journal of Innovations in Engineering and Technology (IRJIET)

ISSN (online): 2581-3048

Volume 9, Issue 8, pp 75-80, August-2025

https://doi.org/10.47001/IRJIET/2025.908010

Radial velocity in the 225 km range is seen in the figure, which is shown at 1 km height. The picture shows a section of wall clouds with a round eye structure.

d) Max_V (Maximum Velocity)

With the exception of using a color scale to display radial velocity, this product's methodology is identical to Max_Z's. The Max_V picture may be used to study the velocity distribution at different locations and angles.

Since the wind is blowing in the same direction at both ends of the radar beam, the radial velocity in the eye remains constant during wind circulation. In the cyclone's wall cloud zone, high winds of around 57 m/s are seen. You may estimate the winds beyond that area by looking at the color table for the velocity scale, but beyond that, they rapidly decrease.

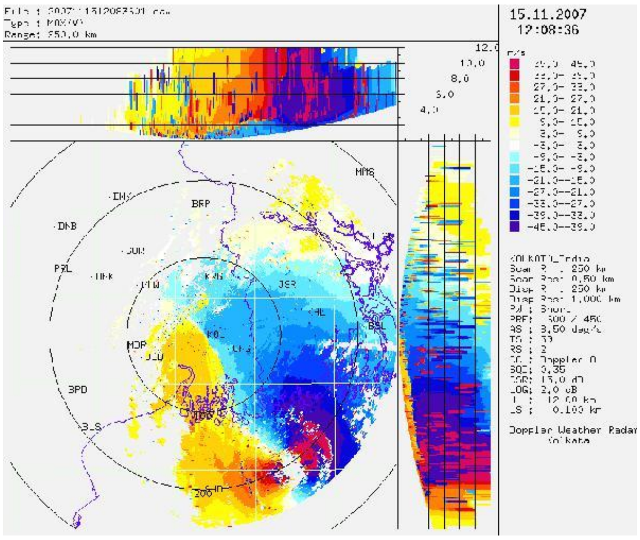

Figure 6: (15.11.2007 / 1200 UTC)

e) VCUT_V (Vertical Cut Velocity)

The VCUT reflectivity imaging algorithm is identical to this product. The radial velocity's vertical cross section is shown by this velocity product.

In relation to the radial velocity the vertical cross-section of the cyclone's eye. In the cloud wall region, high winds of around 51 m/s are visible in the adjacent color presentation, while the wind-free area displays the eye diameter. For estimating the cyclone's strength in relation to eye diameter (where intensity is inversely proportionate to eye diameter) and strong winds, this product is beneficial.

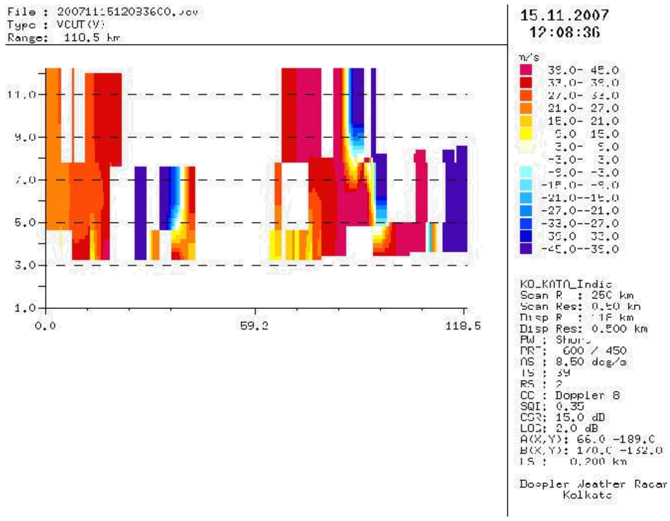

Figure 7: (15.11.2007 / 1200 UTC)

f) VVP_2 (Volume Velocity Processing 2)

This product provides a vertical profile of horizontal winds obtained from radial wind measurements after applying certain approximations and the least square approach to reduce the error. The name of the product itself reveals that the volume velocity data has been processed to produce this product. the expected winds, shown as wind barbs, at intervals of 0.3 km from the ground up to 7.5 km in the air. Because this approach is based on the idea of a linear wind field, the maximum range of the product is 50 km. On the other hand, narrowing the range improves the product's accuracy. Knowing the wind fields at different elevations on the DWR station and the surrounding area is, hence, a great use for this product.

The author conducted research to verify the accuracy of the winds calculated by DWR using data collected from radiosonde flights that were flown from the Met Office in Kolkata, which is 15 km away from DWR. A very strong correlation of the order of 0.85-0.9 was seen at almost all levels of comparison when more than 200 observations were taken during the pre-monsoon season of 2008-2010 across all heights. In addition, VVP_2's display could show a vertical profile over the last six hours or more, allowing you to see how the winds have changed during that time.

VII. CONCLUSION

The author has conducted certain experiments utilizing DWR data, and it seems that the purpose has been attained to a great degree of satisfaction. But based on the findings in this thesis, the author and other scientists will continue to conduct many more investigations along these lines. Understanding the structure and behavior of thunderstorms and tropical cyclones in the Gangetic West Bengal area is made easier with the use of the current study's analytic and statistical methodology.

ISSN (online): 2581-3048
Volume 9, Issue 8, pp 75-80, August-2025
https://doi.org/10.47001/IRJIET/2025.908010

Studies can only be conducted when tornadoes develop near DWR, since their occurrence is quite infrequent in this area. The tornado's development occurred around 220 km from DWR Kolkata, hence the author's research had little to do with tornado features; rather, it focused on identifying important signs of tornado genesis. The funnel-shaped structure that the DWR saw between two clouds at a height of around 16 km and its subsequent decline to 10 km after 20 minutes is a difficult-to-prove precursor to tornado generation. But it does provide light on the ways DWR may be used to learn more about tornadoes and how they form.

REFERENCES

[1] Bhatnagar, A. K., Rajesh, R. P., Kalyanasundaram. S., Thampi, S. B., Suresh, R. and Gupta, J. P. "Doppler radar – A detecting tool and measuring instrument in meteorology", Current Science, Vol. 85(3), 2023.

[2] Bhattacharya, A. K. and Jyoti, P. "Abstraction ratio in the Curve Number method of runoff estimation", Journal of Agricultural Engineering, Vol. 45, pp. 17-22, 2018.

[3] Bhowmik, S. K. R., Roy, S. S., Srivastava, K., Mukhopadhay, B., Thampi, S. B., Reddy, Y. K., Singh, H., Venkateswarlu, S. and Adhikary, S. "Processing of Indian Doppler weather radar data for mesoscale applications", Meteorology and Atmospheric Physics, Vol. 111, pp. 133-147, 2021.

[4] Biggs, E. M. and Atkinson, P. M. "A comparison of gauge and radar precipitation data for simulating an extreme hydrological event in the Severn Uplands, UK," Hydrological Processes, Vol. 25, pp. 795-810, 2021.

[5] Borga, M. "Accuracy of radar rainfall estimates for stream flow simulation", Journal of Hydrology, Vol. 267, pp. 26-39, 2022.

[6] Brian, C. H. and David, C. C. "Integrating radar rainfall estimates with digital elevation models and land use data to create an accurate hydrologic model", Proceedings of the Floodplain Management Association Spring Conference, San Diego, California, 2021.

[7] Carl, L. U., Michael, S., Chad, K., David, C. G., Peter, T., Hoshin, G., Thorsten, W. and Soni, Y. "Real-time flash flood forecasting using weather radar and a distributed rainfall-runoff model", Proceedings of the 2nd Joint Federal Interagency Conference, Las Vegas, NV, 2020.

[8] Chow, V. T., Maidment, D. R. and Mays, L. W. Applied hydrology, McGraw-Hill, New York, 2018.

[9] Chumchean, S., Aungsuratana. P., Khommuang, A. and Hanchoowong, R. "Study of rain-cloud characteristics using weather radar data", 18th World IMACS / MODSIM Congress, Cairns, Australia, 2019.

[10] Collier, C. G. "Flash flood forecasting: What are the limits of predictability?", Quarterly Journal of the Royal Meteorological Society, Vol. 133, pp. 3-23, 2017.

[11] Collier, C. G., Larke, P. R. and May, B. R. "A weather radar correction procedure for real-time estimation of surface rainfall", Quarterly Journal of the Meteorological Society, Vol. 109, pp. 589-60, 2013.

[12] Dalezios, N. R. "Real-time radar rainfall measurements for hydrologic modeling", Ph. D. Thesis, Department of Civil Engineering, University of Waterloo, Ontario, Canada, 2012.

[13] Das, A. "Reverse stream flow routing by using Muskingum models", Sadhana, Vol. 34(3), pp. 483-499, 2019.

[14] Dingman, S. L. Physical hydrology, (2nd ed). Prentice-Hall, Inc, Upper Sattle River, New Jersey, 2022.

[15] Doviak, R. J. and Zrnic, D. S. Doppler radar and weather observations, Academic Press Inc, San Diego, 2013.

Citation of this Article:

Sadhan Biswas, & Dr. Devendra Pradhan. (2025). To Understand the Capabilities of Doppler Radar. *International Research Journal of Innovations in Engineering and Technology - IRJIET*, 9(8), 75-80. Article DOI https://doi.org/10.47001/IRJIET/2025.908010

****

